Titanium oxynitride thin films sputter deposited by the reactive gas pulsing process

Chappé, J.-M.; Martin, N.; Lintymer, J.; Sthal, F.; Terwagne, G.; Takadoum, J.

Published in:
Applied Surface Science

DOI:
10.1016/j.apsusc.2006.12.004

Publication date:
2007

Document Version
Early version, also known as pre-print

Available online at www.sciencedirect.com
ScienceDirect
Applied Surface Science 253 (2007) 5312–5316
applied surface science
www.elsevier.com/locate/apsusc

Titanium oxynitride thin films sputter deposited by the reactive gas pulsing process

Jean-Marie Chappé [a], Nicolas Martin [a,*], Jan Lintymer [a], Fabrice Sthal [b], Guy Terwagne [c], Jamal Takadoum [a]

[a] *Laboratoire de Microanalyse des Surfaces (LMS), Ecole Nationale Supérieure de Mécanique et des Microtechniques (ENSMM), 26 chemin de l'épitaphe, 25030 Besançon Cedex, France*
[b] *Institut FEMTO-ST, UMR 6174 CNRS Département LCEP, 26 chemin de l'épitaphe, 25030 Besançon Cedex, France*
[c] *Laboratoire d'Analyses par Réactions Nucléaires (LARN), Facultés Universitaires Notre-Dame de la Paix, 61 rue de Bruxelles, 5000 Namur, Belgium*

Received 24 October 2006; received in revised form 1 December 2006; accepted 1 December 2006
Available online 8 January 2007

Abstract

DC reactive sputtering was used to successfully make thin films of titanium oxynitride using titanium metallic target, argon as plasma gas and nitrogen and oxygen as reactive gases. The nitrogen partial pressure was kept constant during every deposition whereas oxygen flow rate was pulsed using a square pattern. The study consisted in analysing the influence of the shape of the pulsed rate on physical properties of these films. In order to adjust the metalloid concentration to get films with a wide range of oxygen-to-nitrogen ratios, the reactive gas pulsing process (RGPP) was used. In this process, the oxygen flow switches ''on'' and ''off'' periodically according to a duty cycle $\alpha = t_{ON}/T$. Electrical conductivity of films measured against temperature was gradually modified from metallic ($\sigma_{300K} = 4.42 \times 10^4$ S m^{-1}) to semi-conducting behaviour ($\sigma_{300K} = 7.14$ S m^{-1}) with an increasing duty cycle. Mechanical properties like nanohardness (H_n) and reduced Young's modulus (E_r) of the films were investigated. Experimental values of H_n and E_r obtained by nanoindentation at 10% depth ranged from 15.8 to 5.2 GPa and from 273 to 142 GPa, respectively. Evolutions of H_n and E against duty cycle were similar. A regular decrease was observed for duty cycle $\alpha \leq 25\%$ corresponding to the occurrence of TiO_xN_y phase. Higher duty cycles led to the smallest values of H_n and E and correlated with TiO_2 compound composition. At last, the colour variation of these titanium oxynitrides was investigated as a function of α in the $L^*a^*b^*$ colour space. It was related to the chemical composition of the films.

PACS : 81.15.-z 81.15.Cd

Keywords: Titanium oxynitride; Thin films; Reactive sputtering; Reactive gas pulsing process

1. Introduction

There has been a great scientific interest for metallic oxynitrides for several years, because of their versatile properties [1–4]. They have been prepared by various chemical and physical deposition techniques. Among these types of films, titanium oxynitride films have been one of the most intensively studied systems [5–7]. Recent works on Ti–O–N thin films with a tuneable N/O ratio showed that they exhibit a complex structure and revealed an intermediate behaviour between metallic TiN and insulating TiO_2 compounds [8]. Indeed titanium oxynitrides beneficiate from properties of metallic oxides (colour, optical properties) and nitrides (hardness, wear resistance). Physical vapour deposition and especially reactive magnetron sputtering is an attractive way to deposit these films. A titanium target sputtered in a mixed working gas ($O_2 + N_2$) [9] or the reactive gas pulsing technique [5,10] can be used to modify N/O ratio in the films.

In the present work, we report on physical properties of titanium oxynitride thin films deposited by dc reactive magnetron sputtering. The nitrogen partial pressure was kept constant during every deposition whereas the flow rate of O_2 was modulated periodically. A rectangular wave function with a constant period was used whereas on and off times were

* Corresponding author. Tel.: +33 381402879; fax: +33 381402852.
E-mail address: nicolas.martin@ens2m.fr (N. Martin).

0169-4332/$ – see front matter © 2006 Elsevier B.V. All rights reserved.
doi:10.1016/j.apsusc.2006.12.004

systematically changed. The effects of the oxygen flow modulation pattern on the crystallographic structure, atomic composition, mechanical and electrical properties as well as colour of the films were investigated.

2. Experimental details

A home-made vacuum reactor with a 40 L volume was used to perform the depositions of titanium oxynitride thin films. Substrates were introduced through a 1 L airlock. An ultimate pressure of 10^{-5} Pa was obtained with a turbomolecular pump backed with a mechanical pump. The reactor was equipped with a circular planar and water cooled magnetron sputtering source. The titanium target (purity 99.6%, 50 mm diameter) was dc sputtered with a constant current density $J_{Ti} = 51$ A m^{-2}. The substrates were glass from micro slides and (1 0 0) silicon wafers. Before each run they were ultrasonically cleaned with acetone and alcohol, and the Ti target was pre-sputtered in a pure argon atmosphere for 5 min before introducing nitrogen and oxygen, in order to remove the target surface oxide layer. The substrate was at room temperature and the deposition time was adjusted in order to obtain a thickness close to 400 nm (measured by a mechanical profilometer). Experimental parameters are summarised in Table 1. The shape of the oxygen flow modulation pattern was rectangular. The period T of the pulses and the maximum and minimum oxygen flow rates, q_{O2M} and q_{O2m}, were determined and kept constant (see Table 1) while t_{ON} and t_{OFF} times were systematically changed (Fig. 1). The duty cycle ($\alpha = t_{ON}/T$) was included between 0 and 40% of T, i.e. $t_{ON} = 0$ and 7.2 s. q_{O2M}, q_{O2m} and T were chosen in order to easily alternate the reactive sputtering process between the metallic and compound sputtering mode [10–13].

The elemental analysis of all elements present in the coatings was performed combining Rutherford backscattering spectroscopy (RBS) and nuclear reaction analysis (NRA). In order to analyse the heavy element (Ti) in the coatings, a 3 MeV α particles beam used for the backscattering experiment was produced by the 2 MV Tandetron accelerator installed at LARN in Namur. The scattered particles were detected in a Passivated Implanted Planar Silicon (PIPS) detector placed at 165 ° relative to the incident beam. The analysis of light elements in the coatings was performed with a 5.3 MeV α particles beam produced with the same accelerator. The particles due to

Table 1
Sputtering conditions used to deposit TiO_xN_y coatings

Deposition parameters	
Argon partial pressure (Pa)	0.4
Nitrogen partial pressure (Pa)	0.1
Ti current density J_{Ti} (A m^{-2})	51
Pumping speed (L s^{-1})	24.7
Substrate-target distance (m)	6.5×10^{-2}
Substrate potential	Grounded
Maximum flow rate q_{O2M} (sccm)	1
Minimum flow rate q_{O2m} (sccm)	0
Pulse period, T (s)	18

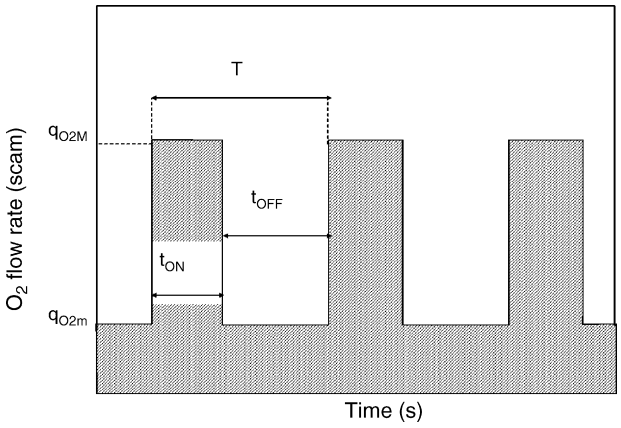

Fig. 1. Schematic representation of pulsed oxygen flow rate: T = pulse period (s), t_{ON} = time of oxygen injection at $q_{O2} = 1$ sccm (s), t_{OFF} = time of oxygen injection at $q_{O2} = 0$ sccm (s), $\alpha = t_{ON}/T$.

$^{14}N(\alpha,p_0)^{17}O$ and $^{14}N(\alpha,p_1)^{17}O$ nuclear reactions were detected in a PIPS detector placed at 90 ° relative to the incident beam. The α scattered particles were stopped in a 24 μm Mylar foil filter located in front of the detector. Simultaneously, the scattered α particles were detected in a PIPS detector at backward angle (165°). At this incident energy, the cross sections of the elastic (α,α) reaction on light elements are non-Rutherford. Data from the literature were used to take into account the true cross sections [14,15] in order to obtain realistic simulation of the experimental spectra.

The crystallographic structure was investigated by X-ray diffraction (XRD) using CuKα radiation at a grazing incidence angle $\theta = 0.7°$. Mechanical properties were investigated performing nanoindentation in dynamic mode with continuous stiffness measurements. A maximum load of 2 mN was applied. Hardness and Young's modulus of the films were determined using a Berkovich nanoindentor. The colour variation of the films was investigated in the $L^*a^*b^*$ colour space with a chromameter.

3. Results and discussion

3.1. Chemical composition and crystallographic structure

Elemental composition measurements carried out by RBS and NRA (Fig. 2) show a reverse and continuous evolution of oxygen and nitrogen atomic concentrations from $TiO_{0.50}N_{1.14}$ for $\alpha = 0\%$ to $TiO_{2.00}N_{0.41}$ for $\alpha = 40\%$. Without oxygen pulsing, titanium nitride films are over-stoichiometric with a N/Ti ratio of 1.14. It is in agreement with a lot of studies and models focused on the reactive sputtering of such compounds [8,16–18]. Nitrogen partial pressure was high enough ($P_{N_2} = 0.1$ Pa) to maintain the process in the nitrided sputtering mode and consequently, TiN films with high nitrogen content were produced. Even for $\alpha = 0\%$, a significant amount of oxygen was detected in the films (close to 19 at.%). It is known that oxygen is always detected in titanium nitride films [8,19] because of the incorporation of oxygen during growth [20] but this amount seems to be quite high. This value could be

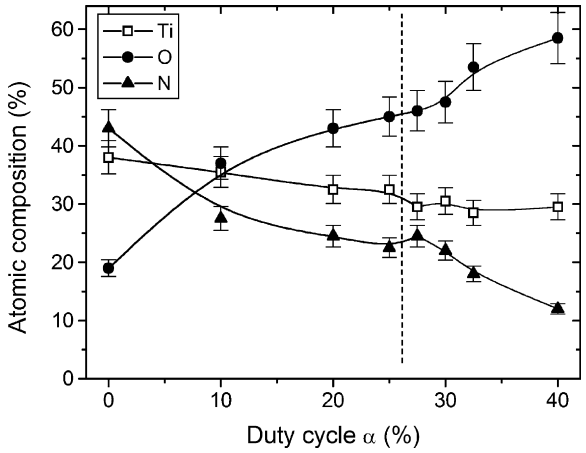

Fig. 2. Influence of the duty cycle α on the chemical composition measured by RBS, of titanium oxynitride thin films.

explained by the diffusion of oxygen evenly through the coating from the surface due to the exposure to the ambient [21]. Then, when α increases, the oxygen content regularly increases from 19 to 58.5 at.% (O/Ti reaches 2.00 for $\alpha = 40\%$) whereas nitrogen concentration decreases down to 12 at.%. Similar results were obtained by Martin et al. [5] about the reverse evolution of oxygen and nitrogen concentrations in titanium oxynitride films by modulation of the oxygen mass flow rate.

X-ray diffraction patterns of the films deposited on (1 0 0) silicon substrates are shown in Fig. 3. The results reveal a strong dependence of the film texture on the oxygen content. For the titanium nitride film ($\alpha = 0\%$), peaks corresponding to the f.c.c. TiN phase appear with a preferential orientation along the (1 1 1) direction. This kind of nano-structured compound, with a crystallite size about 20 nm (revealed by the Scherrer's method), disappears when oxygen is injected ($\alpha > 0\%$). Orange-brownish TiN:O coatings become TiO_xN_y with a dark green colour exhibiting peaks corresponding to f.c.c. structure. TiN and TiO present the same crystallographic structure with neighbour lattice parameters ($a_{TiN} = 4.2417$ Å from P.D.F. 38–1420 and $a_{TiO} = 4.1770$ Å, 8–117). Therefore, X-ray diffraction is not a suitable method to distinguish between both structures. Thus, the right structure of TiO_xN_y thin film cannot be clearly identified. The films may be biphased: a weakly crystallised f.c.c. phase and an amorphous one. When α grows from 5 (Fig. 3b: crystallite size about 15 nm) to 25% (Fig. 3d), the two main peaks corresponding to (2 0 0) and (2 2 0) plans become smaller and disappear when α is too high (32.5%, Fig. 3e): the TiO_2:N films clearly exhibit an amorphous structure.

3.2. Electrical conductivity

The electrical conductivity σ was measured at room temperature for various duty cycles α (Table 2). The electrical conductivity regularly decreases from $\sigma = 4.42 \times 10^4$ to 7.14 S m^{-1}, as α changes from 0 to 25%. Such an evolution is related to the increasing oxygen content in the films and to the change from metallic-like character to a semi-conducting one

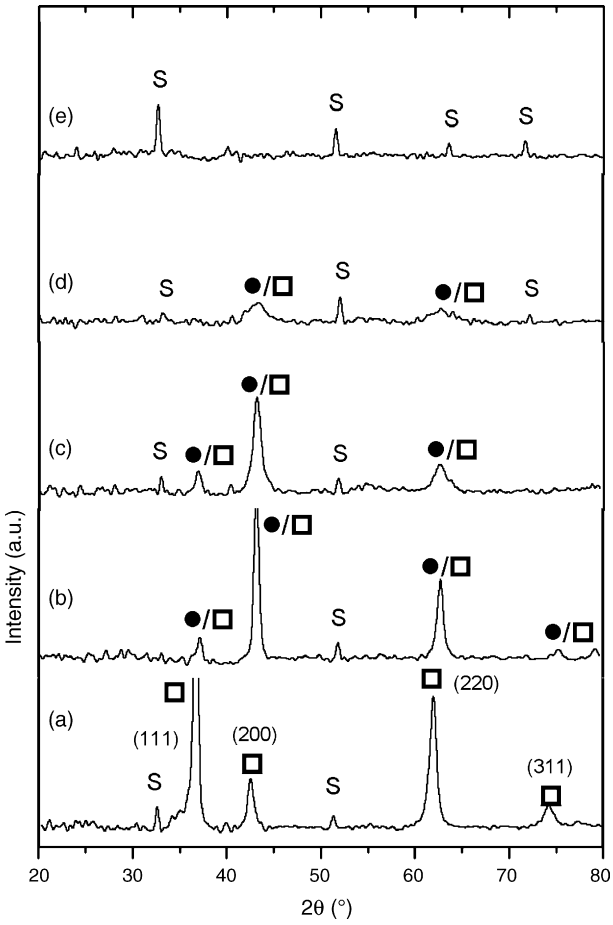

Fig. 3. X-ray diffraction patterns of titanium oxynitride thin films deposited on silicon (1 0 0): (a) $\alpha = 0\%$; (b) $\alpha = 5\%$; (c) $\alpha = 15\%$; (d) $\alpha = 25\%$; (e) $\alpha = 32.5\%$; (□) TiN; (●) TiO; S = substrate.

for oxygen-rich coatings. Electrical conductivity is indicated in Fig. 4 versus the reverse of temperature for α included between 0 and 27.5%. The metallic behaviour of TiN coating prepared without oxygen (decrease of σ when temperature increases) vanishes with the presence of oxygen. A negative slope of log $\sigma = f\ (1000/T)$ is measured and corresponds to a linear behaviour in the Arrhenius plot. The activation energy is then given in Table 2. For $\alpha \leq 15\%$, the slope still exhibits low values ($E_a \leq 88$ meV) indicating that titanium oxynitride thin films with low oxygen contents (lower than 40 at.%) are still

Table 2
Electrical parameters σ and E_a against the duty cycle α

Duty cycle α (%)	Electrical conductivity at room temperature (S m^{-1})	Activation energy E_a (meV)
0	4.42×10^4	–
5	1.56×10^4	–
10	6.59×10^2	45
15	6.00×10^1	88
20	5.08×10^1	176
25	7.14	182
27.5	–	209
28.5	–	282

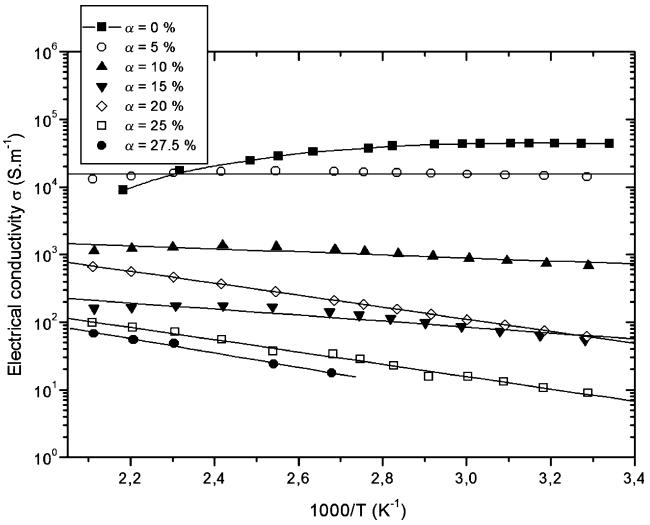

Fig. 4. Electrical conductivity σ vs. $1000/T$ measured on titanium nitride (solid line) and oxynitride thin films for various duty cycles α.

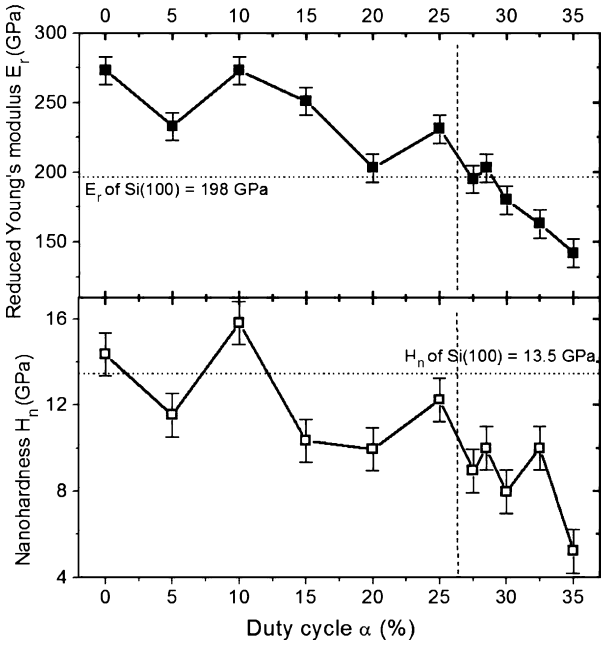

Fig. 5. (a) Reduced Young's modulus E_r and (b) nanohardness H_n of titanium oxynitride thin films against the duty cycle α.

partly metallic. For α higher than 15%, a gradual transition from metallic to semi-conducting behaviours is observed as α increases and the activation energy E_a rises up to 282 meV. This rise correlates with the reverse evolution of oxygen and nitrogen concentrations in the films (Fig. 2). For higher duty cycles, the coatings tend to behave as insulating titanium dioxide compounds. The electrical conductivity is too low and cannot be measured even at high temperature. So, the transition of these titanium oxynitride films from metal to insulator by semi-conductor is clearly demonstrated and seems to be steady as a function of the duty cycle.

3.3. Mechanical properties

The reduced Young's modulus E_r and the nanohardness H_n of the films were obtained by the Oliver and Pharr's method with the unloading stiffness and the real contact area [22]. Indentations were made at 10% depth (i.e. around 40 nm) in order to minimise the influence of the substrate on the final value [23,24]. The evolution of E_r and H_n as a function of α is shown in Figs. 5a and b, respectively. The curves exhibit the same behaviours. For $\alpha \leq 25\%$, E_r slowly decreases from 245 down to 200 GPa and similarly, H_n is reduced from 12.5 down to 10 GPa. For $\alpha \geq 25\%$, E_r and H_n are both significantly reduced (mechanical performances lower than that of Si (1 0 0)). As previously observed from chemical composition and XRD analyses, a duty cycle of 25% seems to be the limit between the metallic conducting hard nitrides and the insulating softer oxides. Besides, 25% is exactly the value of α from which the films become insulating and transparent. It also corresponds to an amorphous structure occurrence (Fig. 3). Here again, the value of $\alpha = 25\%$ corresponds to the significant variations of oxygen and nitrogen concentrations (Fig. 2). The oxygen content increases larger after this limit and tends to the concentration corresponding to TiO_2 compound.

3.4. Colours

The average specular colour of the films deposited on glass is represented in the CIELab colour space [25] in Fig. 6. This graph shows that films are dark golden for $\alpha = 0\%$. They present a very dark green colour for α included between 5 and 15%. Then, they become dark green for $20 \leq \alpha \leq 25\%$, green for $\alpha = 27.5$ to 28.5% and finally light green to yellow-green for high oxygen contents ($\alpha = 30$–40%). This progression is clearly shown in Fig. 7 where only the coordinates a^* and b^* are represented. A loop starts from $(a^*;b^*) = (2.56;1.08)$ for TiN:O to $(-4.98;11.52)$ for TiO_2:N. The lightness is stable before $\alpha = 25\%$ at $L^* = 37$ after which it regularly increases until $L^* = 81$ for $\alpha = 40\%$. It is noticeable that 25% is again the limit between opaque and transparent films. These results prove that

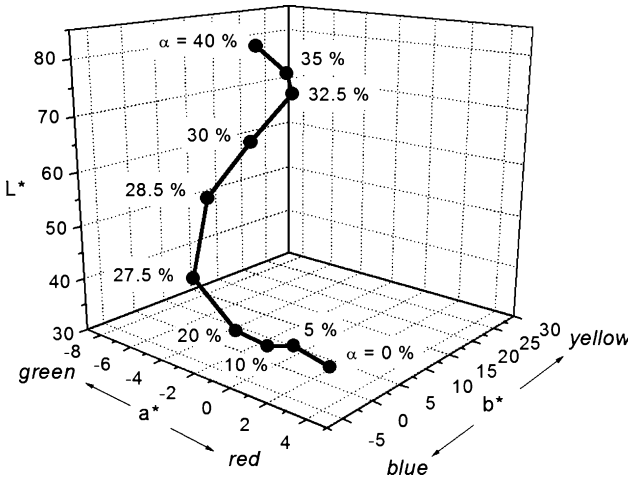

Fig. 6. Average specular colours in the CIELab 1976 colour space of titanium oxynitride thin films for various duty cycles α.

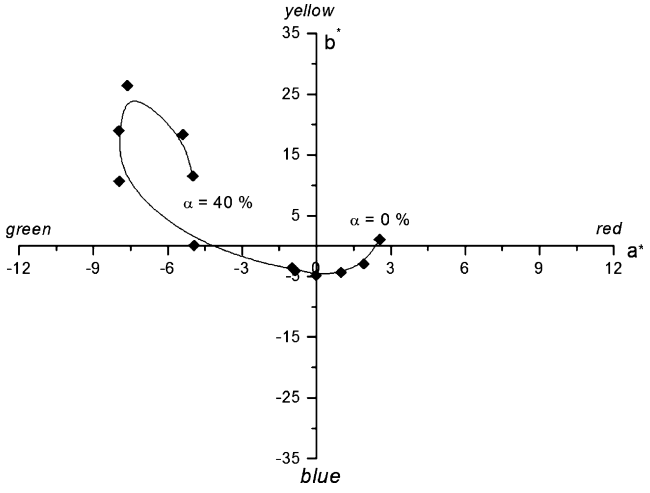

Fig. 7. Projection of the average specular colours in the CIELab 1976 colour space in the a^*b^* plane for titanium oxynitride thin films with various duty cycles α.

it is possible to obtain different shades of green but only this colour is concerned. As a result, some possibilities to produce decorative coatings by varying the duty cycle α or more generally the oxygen flow rate are shown. In addition, such results support that pulsing the oxygen mass flow rate appears as an attractive way to control the optical and decorative performances of titanium oxynitride thin films. Due to drawbacks and typical instability phenomena of the conventional reactive sputtering process and assuming the monotonous evolution of $L^*a^*b^*$ coordinates as a function of α, rectangular pattern is a suitable signal to control the reactive gas pulsing process.

4. Conclusions

The reactive gas pulsing process was successfully used to deposit titanium oxynitride thin films by dc reactive sputtering. An appropriate control of the oxygen flow rate modulation was chosen to deposit titanium nitride (TiN:O), titanium oxynitride (TiO_xN_y) and titanium dioxide (TiO_2:N) coatings. Structural characterisation results revealed a strong dependence of the film structure on the oxygen content. Without oxygen injection, films exhibited peaks corresponding to TiN phase while f.c.c. (TiO and/or TiN) phase was detected for low oxygen contents and films were amorphous for the highest ones. Electrical conductivity measurements of the films revealed a gradual transition from metallic to semi-conducting behaviours as a function of the duty cycle of the oxygen flow rate. Nanohardness measurements showed the softening effect of oxygen on these films and it was correlated with the deposition of amorphous compounds. Regarding colour variations on glass, it can be observed that the dark golden titanium nitride became dark green with increase of oxygen content. They shifted gradually to lighter green and finally transparent yellow-green for titanium oxides. So, the range of intrinsic colours is quite restricted to dark green or violet hues for these parameters. For interferential coatings (duty cycles higher than $\alpha = 25\%$), colours produced could be more interesting on steel substrates or with other parameter variations.

Acknowledgements

The authors gratefully acknowledge the financial support of the European Union through the NMP3-CT-2003-505948 project "HARDECOAT". They also thank Region of Franche-Comté, France.

References

[1] Y. Shima, H. Hasuyama, T. Kondoh, Y. Imaoka, T. Watari, K. Baba, R. Hatada, Nucl. Instrum. Methods B 148 (1999) 599–603.
[2] M. Futsuhara, K. Yoshioka, O. Takai, Thin Solid Films 317 (1998) 322–325.
[3] A.v. Richthofen, R. Domnick, R. Cremer, D. Neuschütz, Thin Solid Films 317 (1998) 282–284.
[4] M. Stavrev, D. Fischer, C. Wenzel, K. Drescher, N. Mattern, Thin Solid Films 307 (1997) 79–88.
[5] N. Martin, O. Banakh, A.M.E. Santo, S. Springer, R. Sanjinès, J. Takadoum, F. Lévy, Appl. Surf. Sci. 185 (2001) 123–133.
[6] F. Vaz, P. Cerqueira, L. Rebouta, S.M.C. Nascimento, E. Alves, P. Goudeau, J.P. Rivière, Surf. Coat. Technol. 174–175 (2003) 197–203.
[7] S.H. Mohamed, O. Kappertz, T. Niemeier, R. Drese, M.M. Wakkad, M. Wuttig, Thin Solid Films 468 (2004) 48–56.
[8] J.M. Chappé, N. Martin, G. Terwagne, J. Lintymer, J. Gavoille, J. Takadoum, Thin Solid Films 440 (2003) 66–73.
[9] F. Vaz, P. Cerqueira, L. Rebouta, S.M.C. Nascimento, E. Alves, P. Goudeau, J.P. Rivière, K. Pischow, L.d. Rijk, Thin Solid Films 447–448 (2004) 449–454.
[10] N. Martin, A.R. Bally, P. Hones, R. Sanjinés, F. Lévy, Thin Solid Films 377–378 (2000) 550–556.
[11] G. Terwagne, J. Colaux, G.A. Collins, F. Bodart, Thin Solid Films 377–378 (2000) 441–446.
[12] D. Gall, R. Gampp, H.P. Lang, P. Oelhafen, J. Vac. Sci. Technol., A 14 (1995) 374–379.
[13] H. Sekiguchi, A. Kanzawa, T. Imai, T. Honda, J. Vac. Sci. Technol. A12 (1994) 3176–3179.
[14] F. Ye, Z. Zhuying, Z. Guoqing, Y. Fujia, Nucl. Instrum. Methods 94 (1994) 11–14.
[15] Z.S. Zheng, J.R. Liu, X.T. Cui, W.K. Chu, Nucl. Instrum. Methods B 118 (1996) 214–218.
[16] L.J. Meng, M. Andritschky, M.P. Dos Santos, Thin Solid Films 223 (1993) 242–247.
[17] J.A. Thornton, J. Vac. Sci. Technol. 11 (1974) 666–670.
[18] S. Berg, T. Larsson, C. Nender, H.O. Blom, J. Appl. Phys. 63 (1988) 887–890.
[19] I. Petrov, L. Hultman, U. Helmersson, J.E. Sundgren, J.E. Greene, Thin Solid Films 169 (1989) 299–314.
[20] F.-H. Lu, H.-Y. Chen, Surf. Coat. Technol. 130 (2000) 290–296.
[21] J. Zhao, E. Gene Garza, K. Lam, C.M. Jones, Appl. Surf. Sci. 158 (2000) 246.
[22] W.C. Oliver, G.M. Pharr, J. Mater. Res. 7 (1992) 1564–1583.
[23] B. Jönsson, S. Hogmark, Thin Solid Films 377–378 (1984) 257–269.
[24] T. Tsui, G.M. Pharr, J. Mater. Res. 14 (1999) 292–301.
[25] R.S. Hunter, R.W. Harold, The Measurement of Appearance, second ed., John Wiley and Sons, New York, 1987.